Preparation and hydrogen storage properties of nanostructured Mg₂Cu alloy

Huaiyu Shao, Yuntao Wang, Hairuo Xu, Xingguo Li*

The State Key Laboratory of Rare Earth Materials Chemistry and Applications, Peking University, Beijing 100871, China

Abstract

We successfully synthesized Mg₂Cu alloys from the metal nanoparticles, which are produced from hydrogen plasma-metal reaction method, in two ways. One is under 0.1 MPa argon at 673 K and the other is under 4.0 MPa hydrogen at 673 K. The structure, morphology and reaction mechanism were studied. The hydrogen absorption and the pressure-composition isotherm properties of the obtained Mg₂Cu alloy under hydrogen were studied. The van't Hoff equation and the formation enthalpy and entropy of the resulting hydride (MgH₂ + MgCu₂) were obtained from the equilibrium plateau pressures of the desorption isotherms. Nanostructured Mg₂Cu shows excellent hydrogen storage properties because nanostructured materials have more surface area and more defects, which means more nucleation sites with hydrogen, and smaller particles, which means shorter diffusion distance for hydrogen in the alloys particles.

1. Introduction

Mg-based alloys have attracted much interest because of the advantages such as light weight, great abundance and high hydrogen capacity of the hydrides. The hydrogen storage capacities in the common Mg-based hydrides are 3.6 wt% for Mg₂NiH₄, 4.5 wt% for Mg₂CoH₅, 5.4 wt% for Mg₂FeH₆ and 2.6 wt% for Mg–Cu–H system (3MgH₂ + MgCu₂). Among these alloys, Mg₂NiH₄ has been widely studied and there have been thousands of detailed papers on its hydrogen storage properties since Reilly and Wiswall reported the hydrogen storage study of Mg–Ni–H system in 1968 [1]. However there is very little work on the hydrogen storage study of Mg–Cu–H system even while they reported the Mg–Cu–H system earlier in 1967 [2]. Furthermore, there is no paper on the hydrogen storage

study of this system in the past 10 years. The situation is similar in Mg–Co–H system though the hydride Mg₂CoH₅ has a much higher storage content than Mg₂NiH₄. The phenomenon in Mg–Co–H system is due to the especially great difficulty in the synthesis of Mg₂Co. The reason to Mg–Cu–H system may be its limited hydrogen capacity and difficulty in preparation of Mg₂Cu compound. As we know, it is difficult to prepare Mg–M alloys (M = Ni, Co, Cu, Fe) by the conventional melting method because of the large melting point and vapor pressure difference between Mg and M.

We have reported a new method of preparing nanostructured Mg-based hydrogen storage materials [3–7]. Firstly, we prepared metal nanoparticles of Mg, Cu, Fe, Co and Ni, etc. by hydrogen plasma-metal reaction (HPMR) and then we obtained nanostructured Mg₂Ni, Mg₂Co alloys from the metal particles and then studied their hydrogen storage. Here, we present our preparation and hydrogen storage study work of nanostructured Mg–Cu–H system. Compared with the

*Corresponding author. Fax: +86 10 627 65930.

E-mail addresses: shaohuaiyu@sina.com (H. Shao), xgli@pku.edu.cn (X. Li).

conventional results by Reilly and others, though they are very few, there are mainly two great advantages in this work. The first one is that we obtain the alloys in very convenient conditions from metal nanoparticles because of the small size and the large specific surface area of the nanoparticles, which means lower melting points during the alloy synthesis procedure. The other one is the excellent hydrogen storage properties the obtained nanostructured alloys show because the nanostructured materials have more nucleation sites and shorter diffusion distance of hydrogen in the alloy particles. We do not seek to develop a practical hydrogen storage alloy, but rather to obtain some fundamental knowledge of this system and to gain some understanding of the effect of nanotechnology on the preparation and hydrogen storage behavior of the this system.

2. Experimental details

2.1. Preparation of Mg and Cu nanoparticles

A schematic figure of the experiment equipment, which is used to produce the metal nanoparticles by HPMR method, is shown in Ref. [5]. The equipment consists of arc melting furnace with artificial tornado system, water-cooled copper hearth, tungsten electrode, heat exchanger of gas with nanoparticles, particle collector, gas circulation pump and DC source. Mg (Cu) nanoparticles were produced by arc melting about 50 g bulk metal (purity > 99.5%) in a mixture of 50% Ar (99.999%) and 50% H_2 (99.999%) atmosphere of 0.1 MPa. When the arc plasma was generated in a voltage of 25 V and a current of about 200–300 A, the metal sample was melted and nanoparticles were fabricated. The nanoparticles were carried out by circulating gas flow with a rate of 100 l min^{-1} and were trapped on a membrane filter and were taken out from the chamber after an enough passivation procedure by a mixture of argon and air to prevent the nanoparticles from spontaneous ignition.

2.2. Synthesis of Mg₂Cu alloys

A mixture of Mg and Cu nanoparticles in 2:1 molar ratio was immersed in acetone and then mixed by an ultrasonic homogenizer for 30 min (15 min every time, twice). After having dried in the air naturally, the metal mixture was pressed into pellets under a pressure of about 75 MPa by a press for 30 s. The obtained pellets were about 13 mm in diameter and 0.5 mm in height and 0.2 g in weight. The pellets were then crushed into some pieces as the sample (named sample A, hereafter) for the alloy synthesis.

From sample A, we prepared Mg₂Cu alloys in two different ways. One is under argon atmosphere. After

sample A was placed in a tube furnace, the system was evacuated to 0.1 Pa. A flowing argon atmosphere of 0.1 MPa was provided and then the sample was heated to 673 K at a heating rate of about 6 K min^{-1}, kept for 7 h and cooled to room temperature. Then we got sample B. The other is under a high hydrogen pressure atmosphere. After sample A was put into a reactor, the system was evacuated to 10^{-3} Pa. After the sample was heated up to 673 K at a heating rate of about 6 K min^{-1}, a hydrogen pressure of about 4.0 MPa was provided to make the Mg and Cu mixture react with hydrogen for 9 h. After that, the system was evacuated again, kept for 2 h and then cooled to room temperature. Here we got sample C.

2.3. Characterization and measurements

The structural analysis of the samples before and after synthesis reaction was carried out by X-ray diffraction (XRD) using an automatic Rigaku X-ray diffractometer with monochromatic CuKα radiation. The measurements were conducted at a scanning rate of 4°min^{-1} using a generator voltage of 40 kV and a current of 100 mA.

The differential scanning calorimetry (DSC) measurements were carriedout using a NETZSCH DSC 204 HP apparatus. The temperature was gradually increased from room temperature to 823 K at a heating condition of 20 K min^{-1} and then cooled to 323 K at a cooling rate of 20 K min^{-1}, and then the heating and cooling cycle was repeated once. All the measurements were conducted under 4.0 MPa hydrogen pressure. But during the cooling process, the pressure will reduce to a minimum of about 3.3 MPa because of the fast cooling rate and the high heat conductivity of hydrogen. The flow rate was 50 ml min^{-1}.

The size distribution and morphology of samples were observed by transmission electron microscopy (TEM) on a JEM-200CX operating at 160 kV. The hydrogen absorption and pressure-composition isotherm (P–C–T) properties were evaluated by using an automatic apparatus from Suzuki Shokan Co. ltd (Japan). The hydrogen absorption measurements were conducted under a starting hydrogen pressure of about 3.0 MPa and an ending pressure of about 2.8 MPa at 523, 548, 573, 598 and 623 K. The isotherm measurements were operated in the hydrogen pressure range from 0.01 to 4.5 MPa at 573, 598 and 623 K.

3. Results and discussion

3.1. XRD patterns, DSC curves and reaction mechanism

XRD results of the different samples are shown in Fig. 1. Fig. 1(a) is the mixture of Mg (JCPDS 35-0821,

hexagonal, space group: $P6_3/mmc$, $a = 3.214$ Å, $c = 5.211$ Å) and Cu (JCPDS 04-0836, cubic, space group: $Fm3m$, $a = 3.615$ Å) nanoparticles. Actually, there should be a very weak peak observed at $2\theta = 42.8°$ corresponding to the MgO phase [6] in Mg phase. But here this peak is not obvious in the mixture because of the high diffraction intensity of Cu phase under $CuK\alpha$ radiation. The MgO phase was formed when the Mg nanoparticles were passivated with air. The thin MgO layer in the surface of the Mg nanoparticles can effectively prevent the Mg particles from further oxidation. The situation is different in the case of Cu nanoparticles. During the HPMR and the passivation process, the Cu nanoparticles are not easily oxidized. But the Cu can be oxidized slowly and later in the next several months. Fig. 1(b) shows the XRD result of sample B—the Mg_2Cu sample synthesized under 0.1 MPa argon. There are two main phases in sample B: Mg_2Cu (JCPDS 13-0504, orthorhombic, space group: $Fddd$, $a = 9.102(1)$ Å, $b = 18.198(1)$ Å, $c = 5.278(1)$ Å) and $MgCu_2$ (JCPDS 01-1226, cubic, space group: $Fd3m$, $a = 7.051(1)$ Å). Mg_2Cu is the main phase and the impurity of $MgCu_2$ phase is about 15%. We can still find some Mg and Cu peaks in this curve. Though there seems to be some exciting results of preparing Mg_2Cu alloys [8], we find that it is not easy to obtain pure

Fig. 1. X-ray diffraction patterns of (a) Mg and Cu nanoparticle mixture (sample A), (b) Mg_2Cu sample produced under argon (sample B), (c) Mg_2Cu sample produced under hydrogen (sample C), (d) hydride sample after hydrogen absorption of sample C.

Mg_2Cu compound from metal nanoparticles in such convenient conditions (0.1 MPa argon, 673 K, 7 h). When we adjust the sintering time or the sintering temperature, we will always meet one of the situations: either more Mg and Cu will be left or more $MgCu_2$ impurity will be yielded. We obtained the better result—sample C when we prepared the Mg_2Cu alloy under 4.0 MPa hydrogen atmosphere at the same temperature (Fig. 1(c)). The yield of Mg_2Cu is higher than 90%. The lattice parameters of Mg_2Cu in sample C are $a = 9.102(1)$ Å, $b = 18.198(1)$ Å, $c = 5.279(1)$ Å and the lattice parameter of $MgCu_2$ is $a = 7.051(1)$ Å, which are almost the same as those in sample B. We meet the similar problem of more metal phase left or more $MgCu_2$ yielded in adjusting the sintering time or temperature to lower the impurity content of $MgCu_2$ in sample C. All the hydrogen property measurements were carried out using sample C. Fig. 1(d) is the result after the hydrogen absorption of sample C. We can find MgH_2 (JCPDS 12-0697, tetragonal, space group: $P4_2/mnm$, $a = 4.518$ Å, $c = 3.021$ Å) and $MgCu_2$ phases in the pattern.

The synthesis reaction mechanism of the Mg_2Cu in sample B (0.1 MPa argon pressure, 673 K, 7 h) is very simple. It will be

$$2Mg + Cu \rightarrow Mg_2Cu. \tag{1}$$

The reaction mechanism of the Mg_2Cu in sample C is a bit complex. We should turn to the DSC results to look for more details. Fig. 2(a) and (b) are the DSC results of the samples starting from Mg nanoparticles and sample A (2Mg + Cu nanoparticle mixture), respectively. From Fig. 2(a), we can see that at the first heating cycle, there is an obvious exothermic peak at 663 K and several small exothermic peaks from 718 to 762 K, which are enclosed in the ellipse. These peaks correspond to hydrogen absorption reaction (Eq. (2)).

$$Mg + H_2 \rightarrow MgH_2, \tag{2}$$

$$MgH_2 \rightarrow Mg + H_2. \tag{3}$$
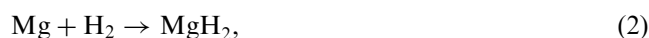
There is one big exothermic peak during the first cooling cycle in Fig. 2(a). This peak is also due to Eq. (2). During the first heating cycle, only partial Mg sample reacts with hydrogen to form the hydride because it is difficult for hydrogen to penetrate the MgO layer on the surface and enter the Mg particle interior. After the particle surfaces are cracked because of the entry of the hydrogen, much fresh surface comes into being and it will be easier for hydrogen to enter the particle interior and react with the left Mg to form MgH_2. At the second heating and cooling cycle, there is one endothermic and exothermic peak at 745 and 674 K, respectively. The endothermic peak at 745 K is due to the hydrogen desorption reaction (Eq. (3)) of the hydride. After the hydride MgH_2 desorbs hydrogen
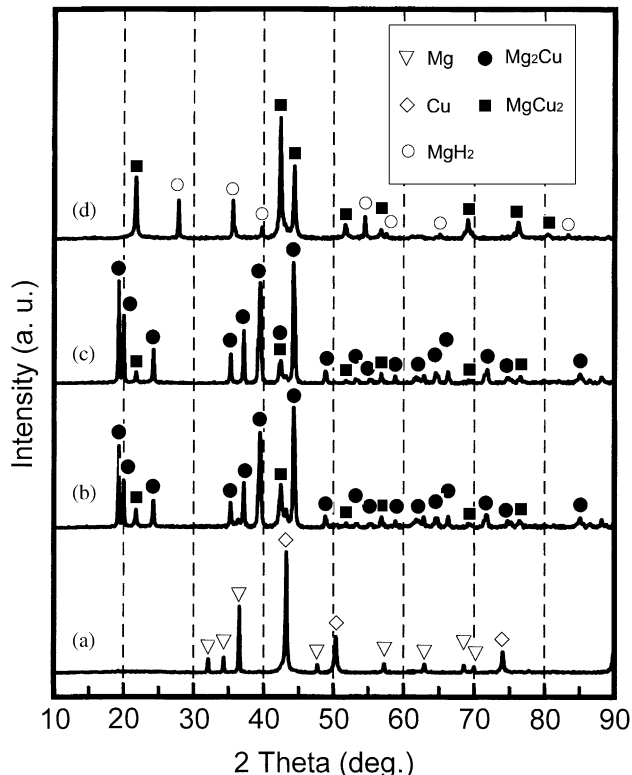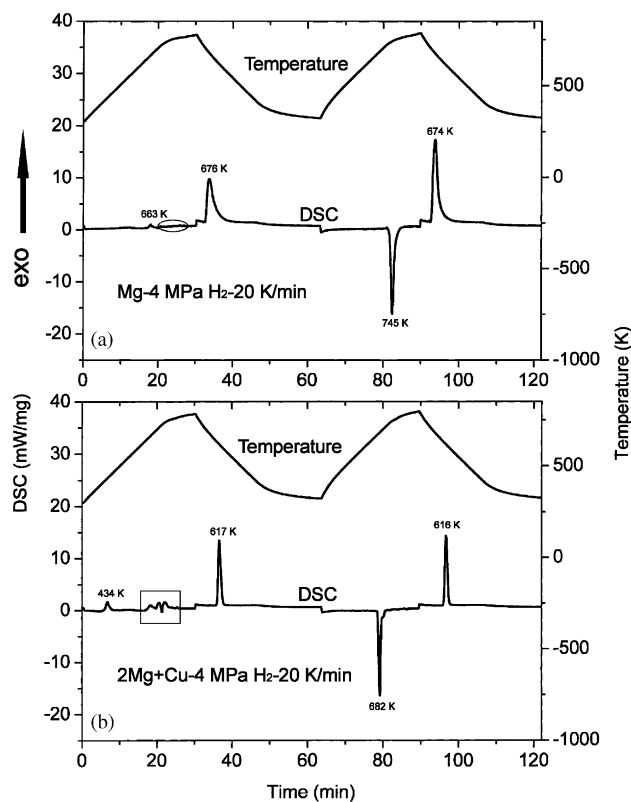
Fig. 2. DSC curves of (a) Mg nanoparticles and (b) Mg and Cu nanoparticle mixture (sample A).

and forms Mg, the produced Mg absorbs hydrogen again to forms hydride (Eq. (2)), which results in the exothermic peak at 674 K. We can see the great hydrogen kinetics of the Mg nanoparticles from the sharp peak shapes. From Fig. 2(b), we can see that at the first heating cycle under 4.0 MPa hydrogen, the first exothermic peak appears at 434 K. This peak is corresponding to Eq. (2) with Cu nanoparticles as the hydrogen absorption catalyst. Comparing with the first exothermic peak at 663 K in Fig. 2(a) due to the same reaction, we can see the excellent catalytic effect of Cu. The addition of Cu lowers the hydrogen absorption reaction temperature (peak temperature) about 230 K. We have reported the catalytic effect of Ni and Co to the hydrogen absorption reaction of Mg before [5,7]. After the first exothermic peak, from 664 and 736 K, there are several peaks, which are enclosed in the rectangle. It is difficult to define the exact reaction mechanism of each peak. However, during the next cooling period there is only one exothermic peak, which is at 617 K. This peak is ascribed to the hydrogen absorption of Mg_2Cu alloy, which can be confirmed by the pressure and temperature results of the P–C–T curves shown later. This means there is no unreacted Mg phase in the sample after the first heating process, otherwise there will be an exothermic peak at about 676 K as in Fig. 2(a). Considering the XRD results and DSC results, we can

get the possible reactions of the peaks enclosed in the rectangle. They should be Eqs. (1), (2) and (4):

$$2MgH_2 + Cu \rightarrow Mg_2Cu + 2H_2. \tag{4}$$
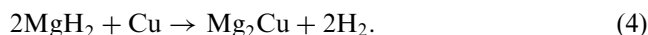
The exothermic peak at 617 K in the first cooling cycle and the one at 616 K in the second cooling cycle are both due to Eq. (5). This can be confirmed by the XRD measurements of the DSC samples after each cooling cycle. We always get the mixture of MgH_2 and $MgCu_2$ from these DSC samples, same as in Fig. 1(d). The endothermic peak at 682 K in the second cycle is ascribed to Eq. (6)—the reverse reaction of Eq. (5). We found the same hydrogen reaction mechanism of Mg_2Cu alloy from other's work here [2,9–11]. The peaks in Fig. 2(b) are sharper than those in Fig. 2(a), which shows the better hydrogen sorption kinetics of Mg_2Cu than Mg.

$$2Mg_2Cu + 3H_2 \rightarrow 3MgH_2 + MgCu_2, \tag{5}$$

$$3MgH_2 + MgCu_2 \rightarrow 2Mg_2Cu + 3H_2. \tag{6}$$
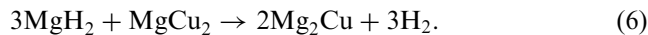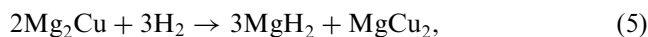
3.2. TEM observation

The Mg nanoparticles are hexagonal in structure and the average particle size is about 300 nm (Fig. 3(a)). The Cu nanoparticles have a granular structure and particle size ranges from several nanometers to 80 nm and the average size is about 40 nm (Fig. 3(b)). The Mg nanoparticles are bigger than the Cu ones and the situations are similar in Mg–Ni [5] and Mg–Co [7] systems. It is because of the higher generation rate of Mg than Ni, Co and Cu by HPMR method, which has been discussed by Ohno et al [12]. Fig. 3(c) shows the obtained Mg_2Cu alloy (sample B) from sample A under 0.1 MPa argon atmosphere, at 673 K and for 7 h. The inserted electron diffraction pattern that has been successfully labeled confirms that the particles are Mg_2Cu compound. The average particle size is about 300 nm because the Mg nanoparticles and Cu nanoparticles react to form Mg_2Cu (Eq. (1)) directly in argon. Fig. 3(d) shows the obtained Mg_2Cu nanoparticles (sample C) from sample A under 4.0 MPa hydrogen pressure, at 673 K and for 9 h. The electron diffraction pattern confirms that the particles are Mg_2Cu. The Mg_2Cu nanoparticles ranges from several nanometers to about 200 nm and the mean particle size is about 100 nm, which is smaller than that of the original Mg particles. This phenomenon also happens in Mg–Ni and Mg–Co systems. The reason is that the particles expand when heated and disintegrate into smaller ones because of the entry of hydrogen during hydrogen absorption and desorption cycle. The Mg_2Cu nanoparticles are bigger than the Mg_2Ni ones. There are two explanations for this. One is the great difference of catalytic effect of
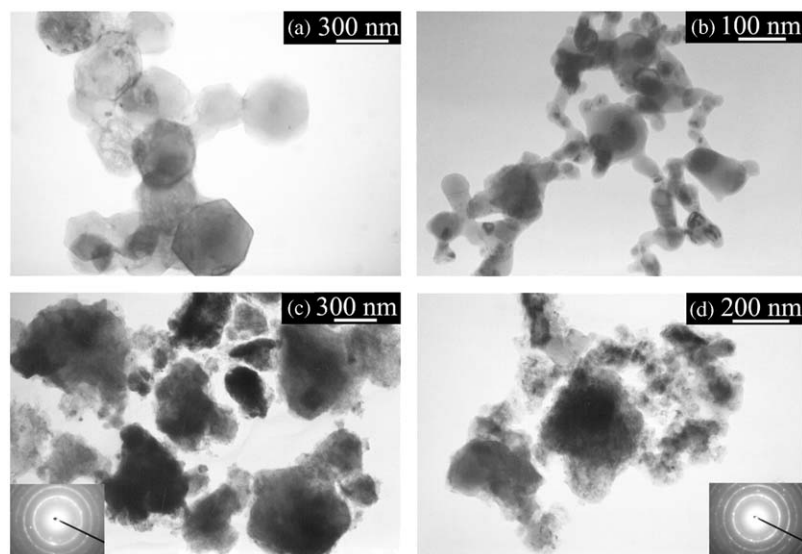
Fig. 3. Bright-field electron micrographs of (a) Mg nanoparticles, (b) Cu nanoparticles, (c) Mg_2Cu produced under argon and (d) Mg_2Cu produced under hydrogen (inset: electron diffraction patterns).

Cu and Ni in the preparation of the alloys. The second one is the difference in the synthesis conditions. The Mg_2Cu alloy is synthesized in a higher temperature for a longer time (673 K, 9 h) than the Mg_2Ni alloy (623 K, 2 h).

3.3. Hydrogen storage properties

Fig. 4 shows the hydrogen absorption curves of the obtained nanostructured Mg_2Cu alloy (sample C) at different temperatures (523, 548, 573, 598 and 623 K) under a starting hydrogen pressure of about 3.0 MPa and an ending pressure of about 2.8 MPa without any activation process. From the figure, we can see that at 523 K, the Mg_2Cu absorbs hydrogen at a slow rate and reaches about 0.63% hydrogen content at the end of the measurement. At the beginning of the hydrogen absorption curve at 548 K, there is a short moment (0–40 s) where the rate is not fast, but after that the sample absorbs hydrogen at a much higher rate. After the measurement, the hydrogen absorption content is about 2.12%. The sample absorbs hydrogen at an excellent kinetics at 573 and 598 K. The absorption content after the measurement is about 2.06%. The hydrogen absorption measurement at 623 K in curve e is a little interesting. Among these several measurement, 623 K is the highest temperature and the most excellent kinetics should be expected here. But actually the absorption rate is slower than those at 548, 573 and 598 K. This phenomenon should be ascribed to the thermodynamic factor. The hydrogen pressure of the absorption measurement is about 3.0–2.8 MPa, which according to the later P–C–T results is the approximate value of the absorption equilibrium pressure of the
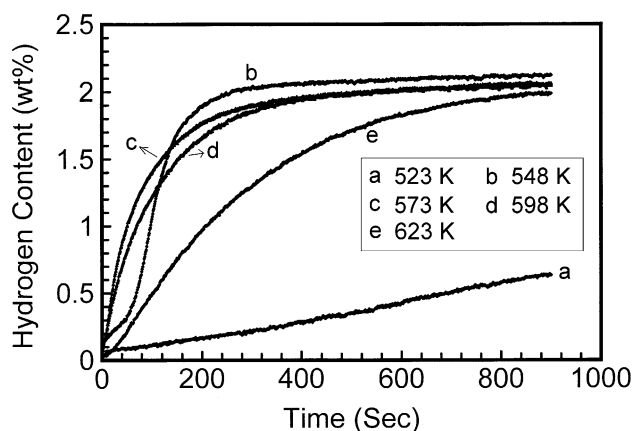

Fig. 4. Hydrogen absorption curves of the nanostructured Mg_2Cu alloy (sample C) under a starting hydrogen pressure of 3.0 MPa at 523, 548, 573, 598 and 623 K.

Mg_2Cu alloy at 623 K. This means the absorption reaction is near an equilibrium period, which results in the not quite fast absorption rate. From this result, we can see that nanostructured Mg_2Cu alloys for hydrogen storage show excellent properties in absorbing hydrogen. There are two reasons for the maximum hydrogen absorption content to be lower than the theoretical value of 2.6%. One is that the sample (sample C) contains some $MgCu_2$ impurity, which cannot absorb hydrogen in these conditions. The other is that the measurement is carried out for only 900 s, but it does not mean that the hydrogen absorption reaction completely finishes after the measurement. After the 900 s measurement, the sample can still absorb some hydrogen despite a much slower rate. The nanostructured alloys show great absorption properties here. The excellent property

is due to more nucleation sites and shorter diffusion distance of hydrogen in the particles the nanostructured alloys provide. We have discussed in detail before. But unlike our nanostructured Mg–H and Mg$_2$Ni–H work published before, on which we can easily find some hydrogen absorption data of conventional bigger powders to compare with, we cannot find any such data on Mg$_2$Cu alloys in literature to compare with.

Fig. 5 shows the P–C–T curves of the hydrogen absorption–desorption for Mg$_2$Cu alloy (sample C) at different temperatures (623, 598 and 573 K). There is one absorption equilibrium plateau and one desorption equilibrium plateau due to the transformation reaction between Mg$_2$Cu and the hydride (MgH$_2$ + MgCu$_2$ mixture) at each temperature. In Table 1, we present the P–C–T characteristics of the nanostructured Mg$_2$Cu alloy at different temperatures. The hydrogen absorption contents are 1.98%, 2.15% and 2.26% and about 99.3%, 94.0% and 93.8% of the absorbed hydrogen can be desorbed during desorption process at 623, 598 and 573 K, respectively. The width of the plateau becomes wider with decreasing temperatures, which is a typical shape in the P–C–T curves of hydrogen storage alloys. The desorption equilibrium plateau pressures are about 1.528, 0.805 and 0.406 MPa at 623, 598 and 573 K, respectively. From the desorption plateau pressures of different temperatures, we can get the van't Hoff

equation expressed by $\ln p$ versus $1/T$. More introduction about van't Hoff equation can be found here [13]. Because of the temperature variation from the set temperatures in the measurement system and to seek more precise results, we use the experimental temperatures at mid-desorption curves when calculating the equation. From the equation, we can figure out the formation enthalpy and entropy of the hydride. Here according to the desorption equilibrium pressures, the van't Hoff equation for the nanostructured Mg$_2$Cu alloy is $\ln(P/0.1\,\text{MPa}) = -9275/T + 17.61$. The formation enthalpy (ΔH) and entropy (ΔS) for the MgH$_2$ + MgCu$_2$ system are -77.11 kJ/mol H$_2$ and -146.4 J/(K mol H$_2$), which agree well with Reilly's [2]. We present the van't Hoff equation plot of the MgH$_2$ + MgCu$_2$ system in Fig. 6 and we also show the former results of several nanostructured hydride systems here. The slope values of the desorption van't Hoff equations indicate the stabilities of the hydride systems. From Fig. 6, it suggests the following order:

$$\text{Mg}_2\text{CoH}_5 > \text{MgH}_2 > \text{MgH}_2 + \text{MgCu}_2$$
$$> \text{Mg}_3\text{CoH}_5 > \text{Mg}_2\text{NiH}_4. \tag{7}$$
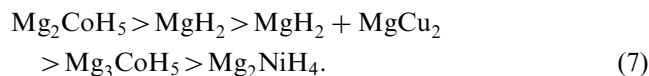
4. Conclusions

The main results are summarized as follows:

1. The Mg and Cu nanoparticles were prepared by HPMR method. From the nanoparticle mixture, we successfully obtained nanostructured Mg$_2$Cu samples from two different ways. One is under 0.1 MPa argon, at 673 K and for 7 h. The other is under 4.0 MPa hydrogen, at 673 K and for 9 h. In both cases, there is some MgCu$_2$ impurity.
2. The Mg$_2$Cu particles prepared in argon have an average size of about 300 nm, while the ones prepared in hydrogen have an average size of about 100 nm. They differ because of the different reaction mechanism. The structure parameters of the obtained Mg$_2$Cu alloys in two ways are almost the same (JCPDS 13-0504, orthorhombic, space group: $Fddd$, $a = 9.102\,\text{Å}$, $b = 18.198\,\text{Å}$, $c = 5.278\,\text{Å}$).
3. The nanostructured Mg$_2$Cu sample prepared in hydrogen can absorb much hydrogen without any
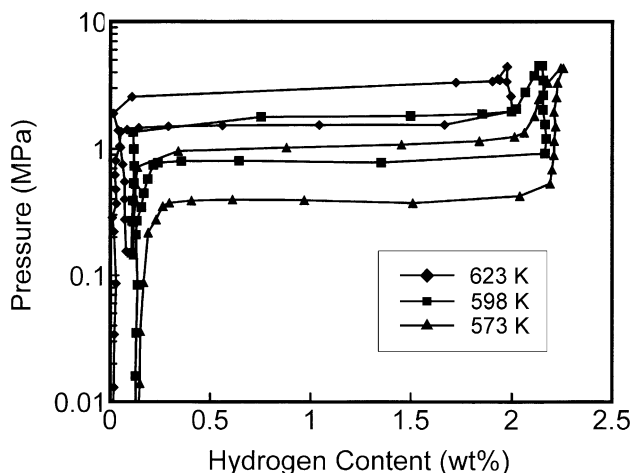

Fig. 5. Pressure-composition isotherm curves of the nanostructured Mg$_2$Cu alloy (sample C) at 623, 598 and 573 K.

Table 1
Pressure-composition isotherm characteristics of the nanostructured Mg$_2$Cu alloy (sample C) at different temperatures

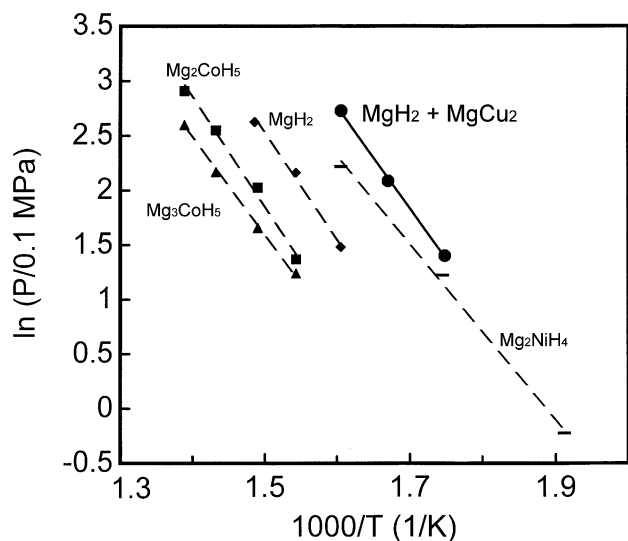|	Hydrogen absorption content (wt%)	% of absorbed hydrogen desorbed	Equilibrium plateau pressure (desorption) (MPa)	Experimental temperature at the mid desorption curves (K)
623 K	1.98	99.3	1.528	622.7
598 K	2.15	94.0	0.805	598.6
573 K	2.26	93.8	0.406	572.0

Fig. 6. Van't Hoff plot for the $MgH_2 + MgCu_2$ system and the former results of Mg_2CoH_5, Mg_3CoH_5, MgH_2 and Mg_2NiH_4 by our group.

activation process at 523, 548, 573, 598 and 623 K under a starting hydrogen pressure of about 3.0 MPa. The excellent property is due to the nanostructure of the materials.

4. The P–C–T results show that the hydrogen absorption contents are 1.98%, 2.15% and 2.26% at 623, 598 and 573 K. The desorption equilibrium plateau pressures at these temperatures are 1.528, 0.805 and 0.406 MPa, respectively.

5. The experimental van't Hoff equation is $\ln(P/0.1 \text{ MPa}) = -9275/T + 17.61$ and the resulting formation enthalpy and entropy for the $MgH_2 + MgCu_2$ system are -77.11 kJ/mol H_2 and -146.4 J/(K mol H_2).

Acknowledgments

References

[1] J.J. Reilly, R.H. Wiswall, Inorg. Chem. 7 (1968) 2254.
[2] J.J. Reilly, R.H. Wiswall, Inorg. Chem. 6 (1967) 2220.
[3] H.Y. Shao, T. Liu, X.G. Li, Nanotechnology 14 (2003) L1.
[4] H.Y. Shao, T. Liu, X.G. Li, L.F. Zhang, Scr. Mater. 49 (2003) 595.
[5] H.Y. Shao, H.R. Xu, Y.T. Wang, X.G. Li, Nanotechnology 15 (2004) 269.
[6] H.Y. Shao, Y.T. Wang, H.R. Xu, X.G. Li, Mater. Sci. Eng. B 110 (2004) 221.
[7] H.Y. Shao, H.R. Xu, Y.T. Wang, X.G. Li, J. Solid State Chem. 177 (2004) 3626.
[8] D.L. Sun, H. Enoki, F. Gingl, E. Akiba, J. Alloys Compd. 285 (1999) 279.
[9] A. Karty, J. Grunzweiggenossar, P.S. Rudman, J. Appl. Phys. 50 (1979) 7200.
[10] A. Biris, D. Lupu, R.V. Bucur, E. Indrea, G. Borodi, M. Bogdan, Int. J. Hydrogen Energy 7 (1982) 89.
[11] P. Selvam, B. Viswanathan, C.S. Swamy, V. Srinivasan, Int. J. Hydrogen Energy 13 (1988) 87.
[12] S. Ohno, M. Uda, Trans. Jpn. Inst. Met. 48 (1984) 640.
[13] G. Sandrock, J. Alloys Compd. 293–295 (1999) 877.